Journal of Structural Engineering & Applied Mechanics (2025) 8(3):200-219
DOI 10.31462/jseam.2025.03200219

RESEARCH ARTICLE

Finite element modeling of a low-rise RC structure for seismic assessment: Validation via operational modal analysis

Merve Bayraktutan[1], Dilek Okuyucu[1*], Sena Refayeli[1], Yusuf Özbağ[1], İbrahim Şahud[1], Kurtuluş Yılmaz[1]

[1] Erzurum Technical University, Department of Civil Engineering, 25100 Erzurum, Türkiye

Article History

Received 23 June 2025
Accepted 14 September 2025

Keywords

Seismic risk assessment
RC building
Dynamic identification
Operational modal analysis
Building stock in Türkiye

Abstract

Türkiye has a large building stock requiring seismic performance evaluation. Law No. 6306, enacted in 2012, governs the identification and renewal of risky structures. In this context, a seismic assessment was conducted on a four-story reinforced concrete building. A finite element model was developed, and theoretical modal analysis yielded a fundamental vibration period of 1.220 seconds. Due to this high value, an operational modal analysis was performed, revealing a period of 0.240 seconds. Comparison with the regional horizontal elastic design spectrum indicated that neglecting the stiffness contribution of infill walls in the model could lead to seismic loads approximately 5.1 times higher than realistic values, which may result in a significantly inaccurate performance assessment.

1. Introduction

Earthquakes are among the most destructive natural hazards affecting human life and the built environment. Türkiye, situated on the active Mediterranean-Alpine-Himalayan seismic belt, is one of the most seismically active countries in the world. In 2023 alone, 62 earthquakes with a magnitude of 5.0 and above were recorded in Türkiye, contributing significantly to the global total of 1,780 such events, including the devastating Kahramanmaraş earthquakes on February 6, 2023 [1-3]. The seismic intensity recorded along the Adıyaman–Antakya corridor reached X–XI on the Modified Mercalli Intensity Scale, with a peak ground acceleration of 1.62g [4]. The enormous impact of these earthquakes, both in terms of loss of life and economic damage, exceeding 150 billion USD, once again highlighted the importance of understanding and accurately characterizing the seismic behaviour of existing structures [5].

Türkiye is a highly earthquake-prone country with a very dense building stock. Many existing structures were constructed before the year 2000, and their seismic safety remains largely unassessed. The year 2000 is a milestone since Türkiye experienced the destructive 1999 Kocaeli-Gölcük earthquakes and took many precautions for new constructions, such as upgrading seismic design codes. In the current situation, systematic seismic performance evaluations are crucial to identify vulnerable buildings and enhance earthquake resilience across urban areas. Finite element modelling is an essential tool in these evaluations, as it allows detailed simulation of structural behaviour under seismic loading. However, the accuracy of such

* Corresponding author (okuyucu@erzurum.edu.tr)
eISSN 2630-5763

models depends heavily on the assumptions made and the need for verification of the structural model with real structural response data, like dynamic behaviour characteristics.

In this context, Operational Modal Analysis (OMA) has become an increasingly popular and valuable technique for evaluating the dynamic characteristics of existing buildings. Due to its non-invasive nature and ability to extract modal parameters under ambient excitation, OMA is particularly suitable for structures that remain in service and cannot undergo forced vibration tests. By providing experimental dynamic data, OMA enables effective calibration of finite element models, improving the reliability and realism of seismic performance assessments. Thus, the combination of finite element modelling and OMA plays a vital role in developing resilient urban environments in earthquake-prone countries like Türkiye.

This study focuses on the application of OMA on an existing four-storey educational building located in Erzurum, a region with a long history of destructive earthquakes, such as those in 1859, 1939, and 1992 [6-8]. Recent studies have demonstrated the increasing use of OMA for calibrating finite element models of existing low-rise reinforced concrete structures. Gültekin and Soyoz [9] performed both experimental and analytical modal analyses on a low-rise reinforced concrete school building and used the OMA results to validate their numerical model. Similarly, Rahmani and Khajehdehi [10] updated the dynamic characteristics of existing RC frames using ambient vibration data. More recently, Demir and Dönmez [11] investigated the seismic behavior of low-rise RC buildings through OMA-based model calibration, highlighting the significant role of infill walls in the global stiffness. These studies emphasize the relevance of OMA in accurately capturing the dynamic behavior of reinforced concrete buildings and support the methodological approach adopted in the present work.

The selected building of this study, consisting of three reinforced concrete floors and a steel-framed top story, was first modelled using finite element methods. Theoretical modal analysis was performed to estimate the building's natural frequencies, mode shapes, and modal periods. However, the initial results indicated that the computed natural period of 1.220 seconds was relatively high for such a low-rise structure, prompting the need for experimental verification. To obtain the building's real dynamic characteristics, field measurements were carried out using high-precision accelerometers placed at designated points throughout the structure. Through the OMA procedure, experimental modal parameters were identified and compared with theoretical predictions. Considerable discrepancies between the theoretical and experimental results emphasized the importance of experimental validation in seismic evaluation processes.

This study mainly concentrates on two main aspects: (1) the implementation of OMA in an existing reinforced concrete building to verify and calibrate the finite element model, and (2) sensor placement optimization to ensure effective and practical modal testing. The findings of this study aim to provide valuable insight for future OMA applications in existing structures located in high seismic risk zones.

2. Material and method

In the presented study, an educational building located within the boundaries of the Yakutiye district of Erzurum was examined. The statements of the owner and users indicate that the construction date of the building is between 1985 and 1986. The educational building in question can accommodate 180 students simultaneously. General views of the building are presented in Fig. 1.

The building consists of a ground floor, two regular floors, and an attic. There is no basement floor. The structure has a reinforced concrete load-bearing system, and there are no shear wall elements in the building. On all floors, the building has a beam-slab system. The ground floor and first floor are used as classrooms, the second floor is used as a cafeteria, and the attic is used as a meeting and resting room. Various interior views of the building are presented in Fig. 2.

(a) (b) (c)

Fig. 1. Various views of the examined educational building: (a) southeast facade; (b) northeast facade; (c) east façade

(a) (b)

Fig. 2. Interior views of the examined building: (a) second floor; (b) first floor

Fig. 3. Attic: Meeting area (Left), Partition wall and roof support system (Right)

The attic is a structure without partition walls, except for external facade walls and the infill wall located to the left of the attic staircase exit. The system, which was later built as a steel structure, consists of roof trusses made of I profiles (IPE200) along the perimeter axes and box-section profiles (50×50×3.2 mm) in the short direction between these profiles. Photographs of the interior of the attic are shown in Fig. 3.

In Türkiye, the seismic performance assessment of the buildings can be legally conducted within the framework of the Law No. 6306 on the Transformation of Areas under Disaster Risk [16]. Pursuant to this law, the seismic performance and risk level of existing buildings are determined based on the guidelines specified in the Regulation on the Principles of Earthquake Risk Determination for Buildings (RYTEIE-2019) [12], which is presented in Appendix 2 of the aforementioned law.

Applications under this regulation must be carried out exclusively by individuals and institutions authorized by the Ministry of Environment, Urbanization, and Climate Change, through the Ministry's official electronic system. Although property owners are granted the right to appeal the outcomes of the seismic performance reports, legal procedures proceed in accordance with the provisions of the finalized report. Accordingly, buildings identified as risky under the RYTEIE-2019 procedure are officially subject to demolition decisions, and the process is formally executed by the competent authorities. Moreover, the government offers specific financial support mechanisms to property owners whose buildings are classified as risky within the scope of Law No. 6306 [13].

In the present study, the finite element model creation of the educational building for the structural performance assessment was exclusively carried out based on the RYTEIE-2019 methodology. Since the building occupants did not consent to excavation works such as the inspection pits typically required for more detailed investigations, alternative evaluation approaches defined in other regulations—such as the Turkish Seismic Code [14]—were not applicable. Given that RYTEIE-2019 does not mandate such invasive procedures, it was deemed the most suitable and practical approach under the circumstances. Furthermore, RYTEIE-2019 has become an increasingly preferred application across Türkiye due to the financial advantages and procedural clarity it offers. This study, therefore, contributes to the current body of knowledge by examining rules of finite element model creation through both theoretical evaluation and practical application.

2.1. Data collection from the building according to RYTEIE-2019

The building under examination is a 4-storey structure, including the attic, and falls under the "Low-Rise Reinforced Concrete Buildings" category according to RYTEIE-2019. The regulations require the determination of the building's structural system characteristics based on surveys of the examination floor and all basement floors. The examination floor is defined as the lowest floor with all facades exposed, throughout the entire floor height. If vertical structural elements (columns or shear walls) are discontinuous or if vertical load-bearing elements rest on beams or coupled columns, a survey must also be conducted on those floors, according to the same regulations. The examined low-rise reinforced concrete building does not have a basement, and only reinforced concrete columns were used as vertical load-bearing elements. In this case, the ground floor was chosen as the examination floor, and separate visual inspections were conducted on each floor for the structural system. The floor height for all floors was measured to be 3 meters. Fig. 4 and 5 present the as-built drawings for the ground floor, second and third floors, and the first floor, respectively.

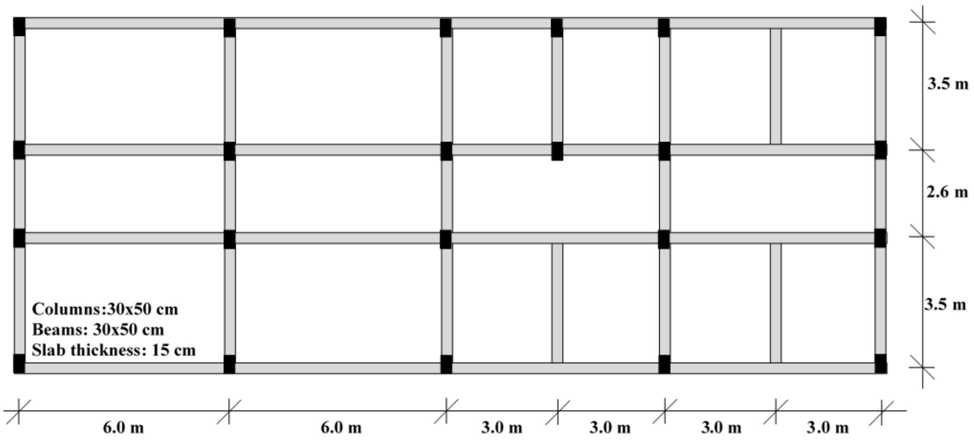

Fig. 4. Survey of the ground and second floors

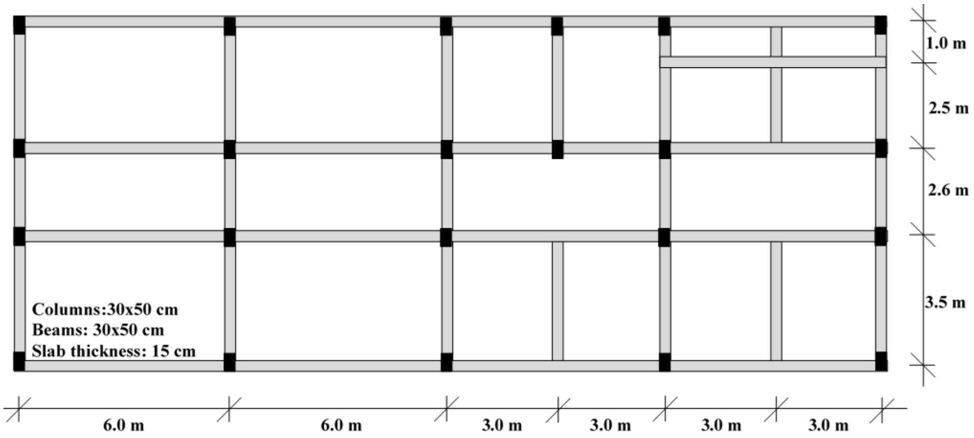

Fig. 5. Survey of the first floor

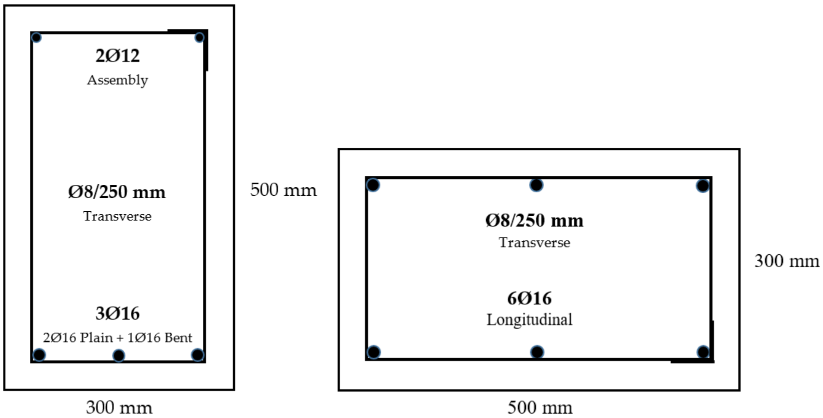

Fig. 6. Reinforced concrete sections determined as a result of the scanning application: Column (Left), Beam (Right)

The columns of the entire structure have a section of 500×300 mm, the beams have a section of 300×500 mm, and the thickness of the beam-slab floor is 120 mm. Since the commonly used reinforcement type in Erzurum in the 1985-1986 period was plain reinforcement, plain reinforcement with a yield strength of 220 MPa was assumed for all the reinforcement. Reinforcement scanning on the floors was used to reveal the reinforcement layout. The primary reinforcement of the slabs was determined to be Ø14/300 mm straight + Ø14/300 mm bent, while the distribution reinforcement was Ø12/150 mm. Column and beam section drawings are presented in Fig. 6.

To define concrete compressive strength, concrete samples were taken as cylinder specimens with a diameter of 65 mm and a height of 65 mm. After necessary corrections are made for size effects, RYTEIE-2019 stipulates that 85% of the average compressive strength value of 10.9 MPa should be accepted as the current compressive strength [12]. In this case, the current concrete compressive strength was determined to be 9.3 MPa.

2.2. Creation of the finite element model according to RYTEIE-2019

Reinforced concrete buildings up to 30 meters high, including basement floors, or buildings not exceeding 10 stories, including basement floors, are defined as Low-Rise Reinforced Concrete Buildings in the RYTEIE-2019 regulations. The studied building does not have a basement floor, and it is a 4-story building consisting of a ground floor, two normal floors, and an added attic. With a total building height of 13 meters, this structure is evaluated as a Low-Rise Reinforced Concrete Building according to RYTEIE-2019. The finite element model of the studied low-rise reinforced concrete building was created using the SAP2000-V21 software [15] according to the rules presented in this section.

In the finite element model created to represent the existing structure, the main components of the building's load-bearing system, such as beams and columns, are modeled using frame elements; the columns are connected to the foundation with fixed supports. The floors are added as shell elements to the model, and in this way, load transfer to the beams and columns is established. Since all floors in the building are 120 mm thick reinforced concrete slab elements, a rigid diaphragm was created in the floors. The column-beam joints are modeled with the existing column and beam stiffnesses without defining rigid regions. Some element joints exhibit a negligible amount of misalignment according to RYTEIE-2019 [12].

The live load on the slabs was assigned as 3.5 kN/m² according to TS 498 [16]. The live load reduction factor of 0.6 was entered into the model for use in the mass source calculation [9]. In the structural system analyses, the effective flexural stiffnesses were used in accordance with RYTEIE-2019. The effective flexural stiffness multipliers for columns and beams were defined as 0.5 and 0.3, respectively, in the model. RYTEIE-2019 has established the calculation of the concrete elasticity modulus using Eq. (1) and the shear modulus using Eq. (2) [12].

$$E_c = 5000\sqrt{f_{cm}} \tag{1}$$

$$G_c = 0{,}40 E_c \tag{2}$$

where f_{cm} is concrete axial compressive strength in MPa, E_c is the modulus of elasticity of concrete in MPa and G_c is the shear modulus of concrete in MPa. Compressive strength of the concrete was determined to be 9.3 MPa on average. As a result of the calculations based on Eq. (1) and Eq. (2), the modulus of elasticity of the concrete was calculated to be 15,248 MPa, and the shear modulus was calculated to be 6,099 MPa. Besides, Poisson's ratio was calculated to be 0.25 using the formula presented in Eq. (3).

$$G_c = \frac{E_c}{2(1+\upsilon)} \tag{3}$$

where υ represents Poisson's ratio. The unit weight of the reinforced concrete element was taken as 25 kN/m³.

RYTEIE-2019 regulations adopt the rule that the contribution of infill walls to lateral stiffness should not be included in the finite element model. In this case, the internal and external infill walls of the structure, constructed with solid bricks, have only been considered as uniformly distributed beam loads in the model. The contribution of the infill walls to lateral stiffness was neglected. The unit weight of the infill wall was considered to be 18 kN/m³. The exterior and interior infill wall thicknesses were determined to be 20 cm and 10 cm, respectively. The corresponding wall loads were calculated to be 10.8 kN/m for exterior walls and 5.4 kN/m for interiors. A general view of the finite element model is presented in Fig. 7.

As a result of the theoretical modal analysis, the first mode shape corresponds to horizontal translational movement parallel to the long plan direction with a period of 1.220 seconds. The subsequent mode shapes involve horizontal translational motion parallel to the short plan direction and lateral torsional movement around the vertical axis. For a low-rise building without reinforced concrete shear walls, a period of 1.220 seconds is considered to be quite high, and therefore, dynamic identification studies were conducted on the structure to experimentally determine the mode shapes and their associated period values. Therefore, OMA was chosen as the preferred method for this study.

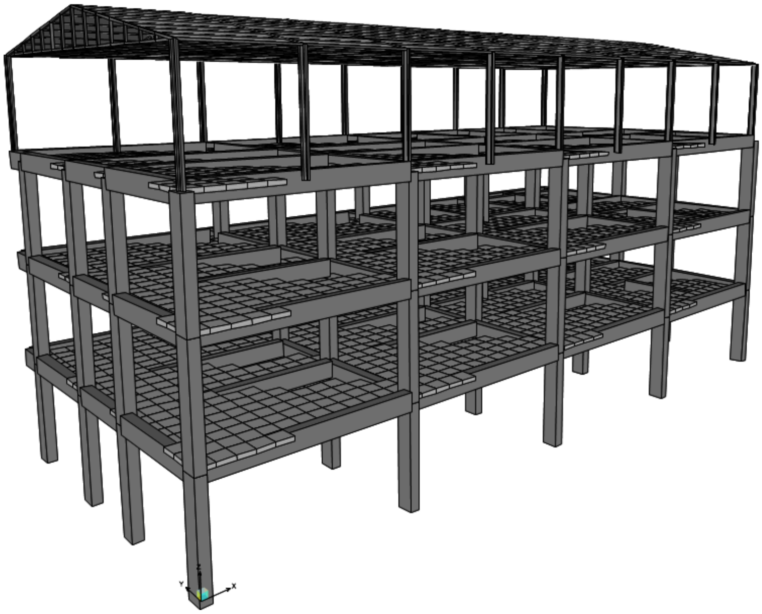

Fig. 7. General view of the finite element model

2.3. Operational modal analysis applications

Every structure responds to the vibrations it is exposed to. These vibrations may be caused by ground (earthquake, vehicle-explosion-induced vibrations, etc.), atmospheric sources (ambient noise, vibrations produced by air traffic, etc.), or usage-based effects. The structure's response to these vibrations can be measured and recorded in terms of displacement, velocity, or acceleration. This data can be analyzed using appropriate methods to obtain the dynamic behavior characteristics of the structure, such as its mode shapes, modal frequencies, and damping ratios. This application, defined as experimental modal analysis, can be performed in two ways based on the excitation source of the structure. The first and most widely used method is Operational Modal Analysis (OMA). OMA is a technique used to non-destructively define the modal characteristics of a structure based on its vibration data under operational conditions. Unlike traditional modal analysis, which requires known artificial excitation, OMA relies on ambient vibrations coming from natural or operational sources. The main goal of OMA is to determine a structure's natural frequencies, damping ratios, and mode shapes. This method is particularly useful for civil engineering structures such as buildings, historical buildings, and bridges, where forced vibration tests may be expensive or destructive. OMA methods can generally be classified into frequency-domain and time-domain approaches, as well as Bayesian and non-Bayesian methods. One of the main advantages of OMA is its economy of application, because it only requires measuring the structure's output vibrations. However, some disadvantages are also noted, such as the potential for significant identification uncertainties due to the need for complex identification methods and the lack of measured loading information [17].

It is possible to state that OMA applications have become widely used in recent years for evaluating the structural integrity and dynamic behavior of various structures in civil engineering projects [18]. OMA is used to monitor the health of structures such as bridges, buildings, and dams. By identifying changes in modal properties (natural frequencies, damping ratios, and mode shapes), it is possible to detect damage or degradation over time. It is well known that important structures around the world are being monitored through OMA applications. Examples of such structures include the Tsing Ma Bridge in Hong Kong with a main span of 1377 meters, and the Cologne Cathedral in Germany [19, 20]. A comprehensive review of OMA studies conducted on bridge structures can be accessed from [20].

The briefly mentioned applications address OMA as a valuable tool in ensuring, assessing, and enhancing the safety, reliability, and longevity of civil engineering structures. As a result of the theoretical modal analysis conducted on the finite element model generated according to RYTEIE-2019, the natural vibration period for the analyzed structure was calculated as 1.220 seconds, and it was found to be relatively high for a 4-storey building. Therefore, it was decided that an OMA application should also be performed on the analyzed structure to experimentally obtain the modal behavior characteristics.

In the first phase of the OMA application, a sensor layout plan was created according to the theoretical mode shapes calculated on the finite element model of the structure, as shown in Fig. 8. Uniaxial accelerometer sensors of high precision were used to measure the building's response vibrations. However, due to the insufficient number of accelerometers available in the inventory to collect data from a total of 40 points simultaneously, the response vibration measurements were carried out using a floating sensor-reference sensor application. The only limitation for this application was not the insufficient number of accelerometer sensors. Another constraint was the number of data logging channels of the portable dynamic data acquisition system, which was 16. In the floating sensor-reference sensor application, reference points where the sensors would remain permanently are first identified. Then, sensor placements for each measurement group are made as planned. After the relevant measurement is completed, the reference sensors are kept fixed, and the existing sensors are shifted. This process is repeated until data collection is completed from all the points where measurements are to be taken [18]. In the analyzed educational structure, the sensors marked with red arrows in Fig. 8 were fixed as reference sensors. Vibration measurements were taken from all floors of the building in a total of 5 sets. Response vibrations were only measured in the horizontal directions from the corner points of the building, and no measurement was made in the vertical direction. The main reason for this is that no mode shape involving vertical displacement motion was found within the first 10 mode shapes calculated in the theoretical modal analysis. Images from the response vibration measurement work are presented in Fig. 9.

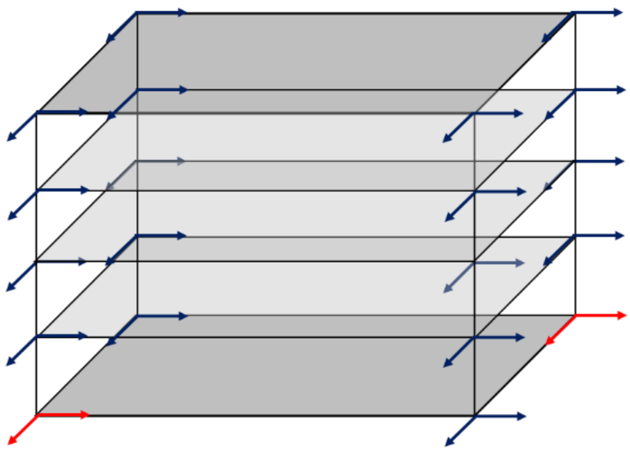

Fig. 8. Accelerometer sensor layout plan for the OMA application

(a) (b)

Fig. 9. Images from the response vibration measurement work within the scope of OMA applications: (a) accelerometer sensors; (b) data acquisition system

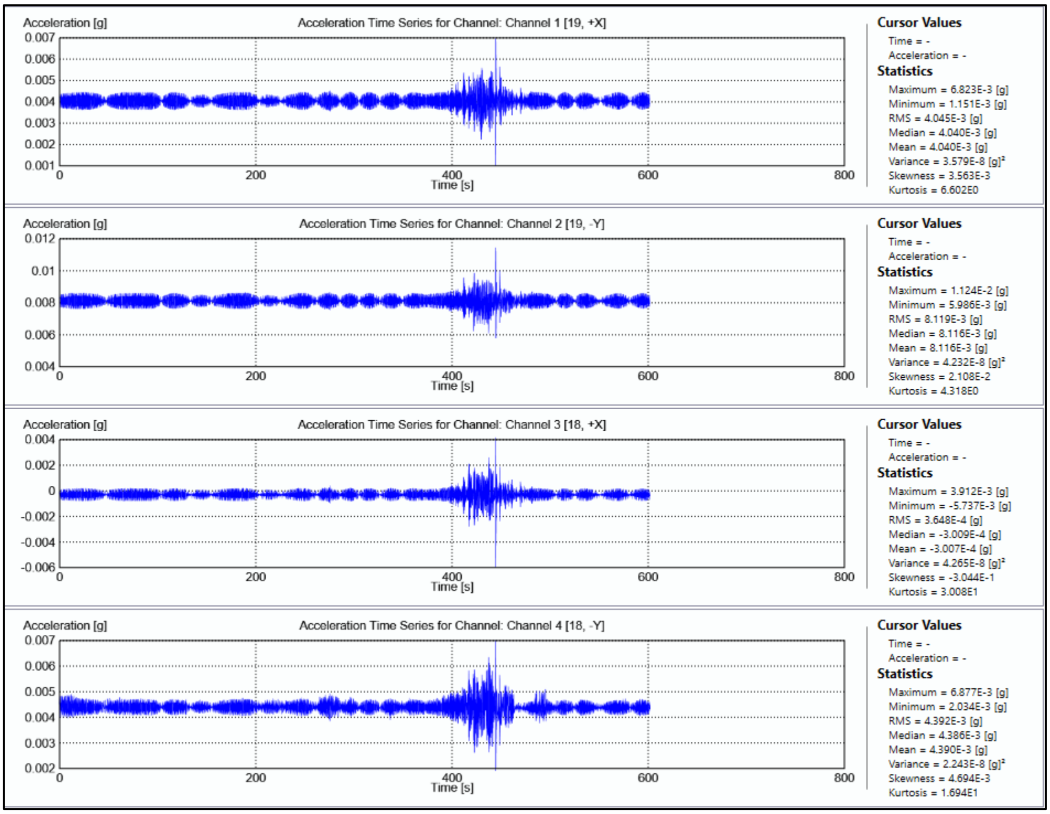

Fig. 10. Response vibration graphs recorded at a frequency of 100 Hz

In the response vibration measurements, a Testbox2010-Field dynamic data acquisition system with 24-bit resolution and 16 channels was utilized. For recording the structural response, Sensebox7021 brand uniaxial wired accelerometer sensors were employed. These accelerometers have a measurement range of ±3 g, a sensitivity of 4.8 V/g, a frequency bandwidth of 4.8 V/g, and an operating temperature range from −40°C to +60°C. The sensors were mounted at the four corners of the reinforced concrete slab on each floor plan. During installation, the sensors were fixed to the measurement points using hot silicone and high-strength adhesive tapes as a precaution against detachment or accidental displacement. Response vibrations were sampled and recorded at a frequency of 100 Hz. Three sets of 10-minute recordings were taken for each floor. It can be stated that the duration of the vibration measurements depends on many parameters, such as the spectral shape and duration of the signal that vibrates the structure, the presence of harmonic vibrations, the complexity of the structure being tested, the quality of the measurement equipment, etc. In the relevant literature, it is suggested that the response vibration measurement duration in OMA applications should be at least 500 times the theoretically calculated natural vibration period [21,22]. Since the natural vibration period calculated on the finite element model is 1.220 seconds, measurements with a duration of 610 seconds (~10 minutes) were taken. A general view of the response vibration graphs recorded at 100 Hz is shown in Fig. 10.

The response vibration data was processed using Artemis Modal Pro (2024) software, and the modal behavior characteristics of the structure were obtained by conducting analyses within the frequency domain [23, 24]. In the case of data analysis of OMA, the geometry representing the structure was first created, measurement data was uploaded to the system, and analyses were then performed. The response vibration data obtained from the structure can be provided to interested researchers upon request.

3. Results and discussions

3.1. Results of theoretical modal analysis

The theoretical modal analysis results calculated on the finite element model that was prepared according to RYTEIE-2019 rules are presented in Table 1. A total of 12 mode shapes were calculated in the theoretical modal analysis, and only the first five mode shapes are presented in Table 1. The main reason for this is that the first five mode shapes could be obtained as a result of the OMA application. It can be stated that the mode shapes calculated by theoretical modal analysis reflect the expected theoretical modal behavior. The first mode shape corresponds to horizontal translational movement parallel to the long plan direction (X), the second mode shape corresponds to horizontal translational movement parallel to the short plan direction (Y), and the third mode shape corresponds to torsional movement around the vertical axis (Z). The period values for these mode shapes were 1.220 s, 0.819 s, and 0.800 s, respectively. The fourth mode shape is a local movement of the roof floor, which was added later to the structure. It was calculated as horizontal translational movement parallel to the long plan direction (X) for the roof floor only. The period value for this mode shape is 0.793 s. The fifth mode shape, calculated with a period of 0.392 s, corresponds to vertical torsional movement of the entire structure around the short plan direction (Y).

Table 1. Theoretical modal analysis results calculated on the finite element model

Mode Number	Mode Shape	Period (s)
1	Horizontal translational movement parallel to the long plan direction	1.220
2	Horizontal translational movement parallel to the short plan direction	0.819
3	Lateral torsional movement around the vertical axis	0.800
4	Horizontal translational movement of the roof floor parallel to the long plan direction*	0.793
5	Vertical torsional movement around the short span direction of the structure	0.392

* Mode shapes related to the local movement of the roof floor itself are explained by italic fonts in this table and beyond.

The order of the first and second theoretical mode shapes might seem surprising. However, looking at the column layout plan, which is the same across all floors, it is observed that all column orientations are identical, and the total column moment of inertia in the short plan direction (6875000 cm^4) is greater than that of the long plan direction (2475000 cm^4). Given that the rigidity effects of the infill walls are not reflected in the finite element model, it is theoretically expected that the first mode shape corresponds to horizontal translational movement parallel to the long plan direction (X), where rigidity is less.

3.2. OMA results

The collected data were analyzed in three different models by using Artemis Modal Pro software, and spectral density functions were calculated. Mode shape estimations were made through these functions, and the corresponding frequency/period values were calculated. Consistency checks of the experimentally obtained mode shapes were carried out using the modal assurance criterion (MAC) values. It can be stated that MAC values are frequently used parameters in the consistency investigations of OMA results [22,25].

The mode shapes and period values obtained from the OMA application are presented in Table 2. As seen, the first experimental mode shape corresponds to the horizontal translational and local movement of the roof floor parallel to the short plan direction (Y). The corresponding period of the first mode shape was calculated to be 0.254 seconds. The second and third mode shapes correspond to the horizontal translational motion of the entire building parallel to the short (Y) and long (X) plan directions, respectively. For the second and third mode shapes, periods of 0.240 seconds and 0.184 seconds were calculated. For the fourth mode shape of lateral torsional movement of the roof floor around the vertical axis, the period was defined to be 0.180 seconds. The fifth mode shape was calculated as a lateral torsional movement around the vertical axis (Z) of the entire building with the corresponding period of 0.174 seconds. A large number of analyses have been performed for the OMA application, and spectral density functions have been calculated. Since it is not possible to present all of them, an example of a spectral density function graph is presented in Fig. 11.

MAC values have been analyzed to assess the reliability and independence of the mode shapes determined from the data analysis of the OMA application. MAC values close to 0 indicate the discreteness of the two mode shapes, while values close to 1 indicate a high degree of similarity. MAC values were calculated for each analysis in the OMA application. The MAC values of the OMA application calculated for the corresponding spectral density function presented in Fig. 11 are shown in Table 3. The MAC values presented in Table 3 compare mode shapes obtained from different experimental setups and are intended to evaluate the consistency of experimental results.

Table 2. Modal behavior characteristics obtained from the OMA application

Mode Number	Mode Shape	Period (s)
1	Horizontal translational movement of the roof floor parallel to the short plan direction	0.254
2	Horizontal translational movement parallel to the short plan direction	0.240
3	Horizontal translational movement parallel long plan direction	0.184
4	Lateral torsional movement of the roof floor around the vertical axis	0.180
5	Lateral torsional movement around the vertical axis	0.174

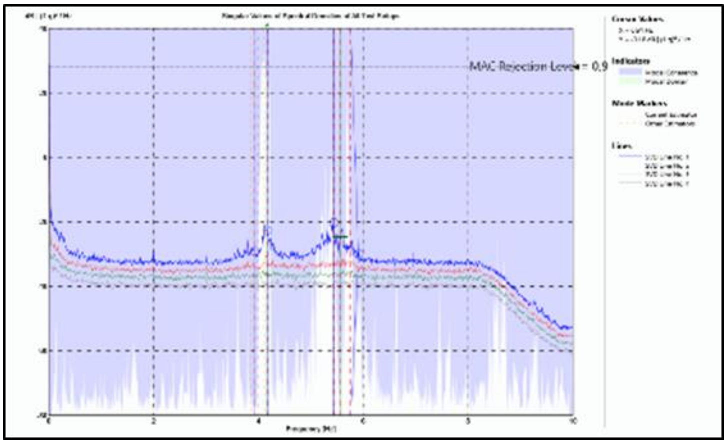

Fig. 11. Spectral density function graph for OMA application

Table 3. MAC matrix calculated for experimental mode shapes

MAC	Mode 1	Mode 2	Mode 3	Mode 4	Mode 5
Mode 1	1	0.7840	0.0024	0.1156	0.1153
Mode 2	0.7840	1	0.0122	0.0231	0.0230
Mode 3	0.0024	0.0122	1	0.3608	0.0191
Mode 4	0.1156	0.0231	0.3608	1	0.4771
Mode 5	0.1153	0.0230	0.0191	0.4771	1

A threshold value of 0.90 was adopted for the MAC during the mode pairing process between theoretical results. This threshold was selected to ensure a high level of consistency between mode shapes, while minimizing the risk of false pairings. Similar threshold values ranging from 0.80 to 0.95 have been widely used in previous studies for reliable mode correlation. The selected value aligns with recommendations found in the literature [26, 27] and provides a balance between sensitivity and robustness in mode matching. MAC value of 0.784 was calculated for the first and second mode shapes as seen in Table 3. This value being close to 1 indicates a high similarity between the mode shapes. Considering that the first mode shape represents the localized horizontal displacement of the roof structure in the short direction, and the second mode shape represents the entire structure's horizontal displacement in the short direction, it is clear that the calculated MAC values accurately represent the behavior. Similarly, for the fourth and fifth mode shapes, the MAC value of 0.477 was calculated. The fourth mode shape represents the localized torsional movement of the roof structure around the vertical axis, and the fifth mode shape represents the entire structure's torsional motion around the vertical axis. In this case, the MAC values also support the conclusion that the related mode shapes are not entirely separate from each other.

An important case observed from the OMA is that, based on the analyses conducted, it was concluded that the structural boundary conditions of the building represented a fixed support behavior. According to RYTEIE-2019, the foundation connection of reinforced concrete buildings in finite element models is typically assumed to be fixed (i.e., fully restrained). In this study, the investigated building does not have a basement; however, response vibration data were recorded from all four corners of the ground floor slab. During data processing, the results obtained from analyses that included the ground floor response data were presented as OMA results. The computed mode shapes showed no noticeable movement at the lowest level of the structure. Additionally, to numerically examine the boundary condition between the structure and the ground, a second set of analyses was conducted in which the ground floor slab response data were deliberately excluded during processing. The mode shapes and period values obtained from this second analysis were found to be identical to those obtained when ground-floor data were included. Based on this result, it was concluded that the assumption of a fixed base in the finite element model is valid for this particular structure, and the interaction between the ground and the building does not significantly affect the modal characteristics observed in the analysis. In other words, as a result of the OMA application, it was found that the assumption of fixed supports in the finite element model, according to RYTEIE-2019, was not incorrect.

3.3. Combined evaluation of theoretical and experimental modal analysis results

The theoretical and experimental modal shapes and period values for the examined structure are presented together in Table 4. It is observed from Table 4 that the modal shapes calculated on the finite element model created according to RYTEIE-2019 differ from those obtained as a result of the OMA application. In the theoretical modal analysis, the first mode shape corresponds to a horizontal translation along the long axis of the structure, while in the OMA application, the first mode shape was determined as a horizontal translation of the recently added rooftop parallel to the short axis of the structure. This observation shows that the OMA application provides insights into the structural health, revealing that the newly added rooftop is not integrated with the existing reinforced concrete structure. As a result of the OMA application, the fourth modal movement corresponded to a local, lateral torsional motion of the roof floor around the vertical axis of the building.

It can be stated that the vibration motion calculated as the first mode shape in the theoretical modal analysis is not surprising for the case where there are no infill walls in the model. When looking at the column layout plan, it is observed that the column directions and numbers are the same on all floors, and the total moment of inertia of the columns in the short direction (6875000 cm^4) is greater than that in the long direction (2475000 cm^4). In this case, it is theoretically expected that the first mode shape would correspond to horizontal translation in the long direction, where the stiffness is lower. However, it should also be noted that the natural vibration period of 1.220 s calculated for the first mode shape in the theoretical modal analysis is relatively high for a 4-storey building. For the investigated structure, the natural vibration period calculated from the finite element model developed according to RYTEIE-2019 is 1.220 seconds, and this value is used as the fundamental vibration period in seismic load calculations in accordance with [12].

If OMA is part of the seismic risk identification process, the first mode shape from the OMA result—representing a local translational movement of the newly added roof with low mass participation—suggests that the second mode shape (0.240 seconds), which corresponds to the building's horizontal translational movement in the short direction, should be considered as the natural vibration mode. It would be considered appropriate to use the period value of 0.240 seconds as the natural vibration period in the earthquake load calculation of the structure. It should be emphasized that the recommendation to use the experimentally identified period value (0.240 seconds) in seismic load calculations pertains specifically to the existing structure examined in this study. This does not imply that theoretically calculated periods are inherently inaccurate or inappropriate for new designs. In the design of new buildings, period estimation formulas—typically based on empirical data and simplified assumptions—offer conservative values that ensure a sufficient safety margin. However, for existing buildings, especially those with non-structural elements such as infill walls contributing significantly to stiffness, using only the theoretical model without calibration may result in substantial deviations from actual dynamic behavior. Therefore, the experimentally obtained period should be considered a more realistic representation of the current condition of the structure, but this does not invalidate the use of code-based period estimations in structural design practice.

Table 4. Results of theoretical and experimental modal analysis

Mode Number	Theoretical		Experimental	
	Mode Shape	Period (s)	Mode Shape	Period (s)
1	Horizontal translational movement parallel to the long plan direction 	1.220	Horizontal translational movement of the roof floor parallel to the short plan direction 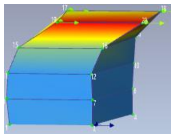	0.254
2	Horizontal translational movement parallel to the short plan direction 	0.819	Horizontal translational movement parallel to the short plan direction 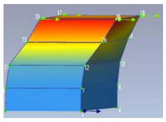	0.240
3	Lateral torsional movement around the vertical axis 	0.800	Horizontal translational movement parallel long plan direction 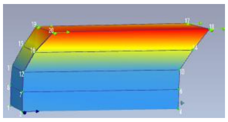	0.184
4	Horizontal translational movement of the roof floor parallel to the long plan direction 	0.793	Lateral torsional movement of the roof floor around the vertical axis 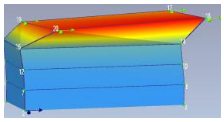	0.180
5	Vertical torsional movement around the short span direction of the structure 	0.392	Lateral torsional movement around the vertical axis 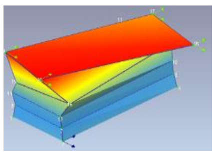	0.174

In both the theoretical and experimental modal analysis results, the second mode shape calculated for both applications was a horizontal translational movement parallel to the short direction of the building. While a period of 0.819 s was calculated theoretically for this movement, the value was determined to be 0.240 s as a result of the OMA application. However, in the OMA application, the second mode shape, which is accepted as the natural vibration motion in terms of mass participation, is a situation that needs further analysis. An important factor that is not reflected in the finite element model under the RYTEIE-2019 rules, but which could affect seismic behavior, is the rigidity effect of infill walls. The exterior walls of the building under study were constructed with 20 cm thick solid bricks, and the interior partition walls were made of 10 cm thick solid bricks. Given the construction year, although hollow bricks were generally used in the construction of infill walls, solid bricks of masonry having very high rigidity were used for infill wall construction. The effects of infill walls on modal characteristics of RC buildings were widely studied in the related literature, providing similar results with herein study [28-31]. As the main conclusion, these rigid infill wall elements should be considered because of their rigidity effects in numerical solutions, and this result is also supported by the other studies [32, 33].

As a result of the evaluation up to this point, it can be concluded that the absence of infill wall stiffness effects in the finite element model created according to RYTEIE-2019 for the analyzed educational structure could lead to results that deviate from the experimentally determined modal behavior. This omission could significantly weaken the model's ability to accurately represent the existing structure and, in later stages of structural analysis, especially for column-beam connections, could lead to incorrect internal force calculations. It is believed that the evaluation of this situation using spectral earthquake forces would be beneficial. The soil at the location of the structure under study is classified as Class B according to TSC (2018) [14]. Class B soils are defined as poorly weathered to moderately hard rocks. In new building designs or performance evaluation studies for existing buildings, horizontal and vertical elastic design spectra based on the geographical location of the building/project and the soil class and provided by the Interactive Earthquake Hazard Map of Türkiye, are used for earthquake load calculations.

The horizontal elastic design spectrum for the building studied is presented in Fig. 12. Two points are marked on the horizontal elastic design spectrum presented in Fig. 12. The first point corresponds to the spectral acceleration coefficient of 0.346, which is associated with the natural vibration period of 1.220 seconds, calculated from the theoretical modal analysis performed on the finite element model created according to the RYTEIE-2019 rules. The other point corresponds to the spectral acceleration coefficient of 1.753, which is associated with the natural vibration period of 0.240 seconds, determined experimentally through OMA application. The spectral acceleration coefficients corresponding to the theoretical and experimental natural vibration periods differ significantly from each other. The spectral acceleration coefficient corresponding to the natural vibration period determined by experimental modal analysis is 5.1 times the spectral acceleration coefficient corresponding to the natural vibration period determined by theoretical modal analysis. This is a remarkable result, meaning that during a ground motion having a spectrum around the design spectra presented in Fig. 12, the spectral seismic load could affect the structure with an impact of 5.1 times that of the theoretical one used in dynamic analysis. A structural analysis using the spectral acceleration coefficient of 0.346, calculated according to RYTEIE-2019, might lead to a decision of continuity of the service and occupation. However, the modal behavior and natural vibration period of the structure determined by OMA applications strongly suggest that the building may perform differently than the performance outlined under the rules of RYTEIE-2019. Therefore, it was concluded that OMA applications are studies that would enhance the safety of evaluations in performance assessment studies of low-rise reinforced concrete buildings under RYTEIE-2019 or other regulations.

The observed discrepancy between the theoretical and experimental fundamental periods may also not be solely attributed to the exclusion of infill wall stiffness. Although the theoretical model neglects the stiffness contribution of infill walls, their mass was still accounted for, which inherently increases the natural period due to added inertia. Furthermore, the effective stiffness factors used in the model are simplified coefficients that may not accurately reflect the complex interaction between the structural frame and infill walls. Boundary conditions, assumed as fixed base in this study, also significantly influence modal properties and may contribute to differences between theoretical and experimental results. To better quantify the effect of infill walls, an additional finite element model including their stiffness was developed. The comparison of modal periods from both models highlights the importance of considering infill walls in seismic performance evaluations of low-rise RC buildings.

In this study, it is evaluated that the discrepancy between the fundamental vibration period calculated from the finite element model developed in accordance with RYTEIE-2019 and the period obtained from the OMA is primarily due to the exclusion of stiffness contributions from the partition walls, which are constructed of solid brick. To further substantiate this assessment, equivalent diagonal struts were incorporated into the finite element model to represent the stiffness of the infill walls, and the theoretical modal analysis was repeated. FEMA 356 recommends the use of the equivalent diagonal strut model to account for the contribution of infill walls to the structural system [35]. In this study, the modeling of infill walls was performed in accordance with the guidelines provided in FEMA 356, where they are represented by equivalent uniaxial compression struts. The finite element model incorporating these equivalent diagonal struts is presented in Fig. 13.

As a result of incorporating the infill wall representation in the finite element model in accordance with FEMA 356 (2000), the fundamental natural vibration period of the structure was calculated as 0.252 s. This value, obtained from the updated finite element model that reflects the stiffness effects of infill walls, is approximately 5% higher than the experimentally derived period of 0.240 s. obtained through OMA. Furthermore, the spectral acceleration coefficient corresponding to 0.252s. The period was found to be 1.676. This value is approximately 0.96 times the spectral acceleration coefficient of 1.753 associated with the experimentally determined period. Based on these findings, it is concluded that incorporating the stiffness of infill walls into the finite element model results in a more accurate estimation of seismic loads for this particular structure.

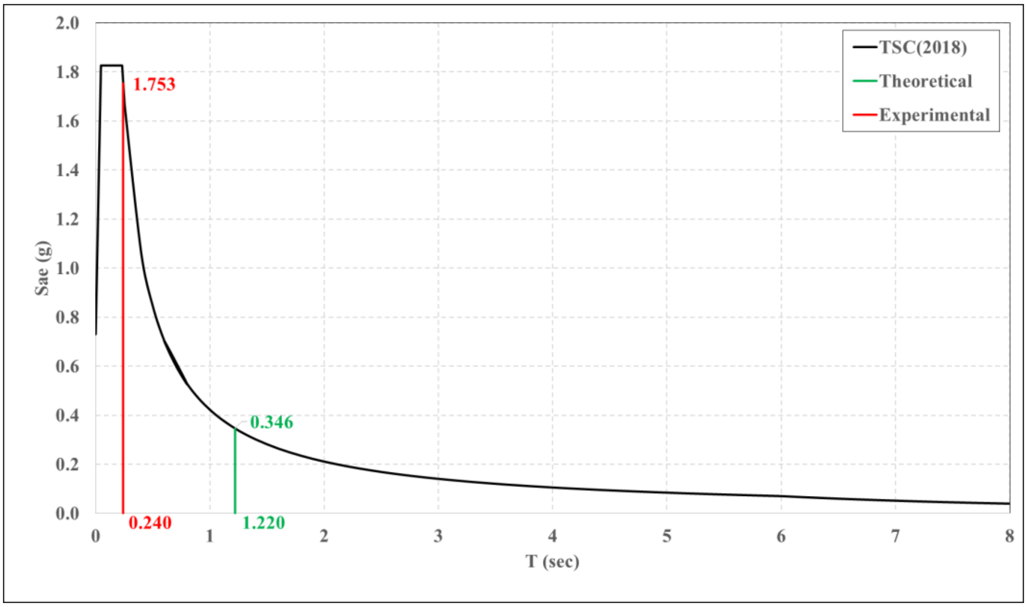

Fig. 12. Horizontal elastic design spectrum for the building studied [34]

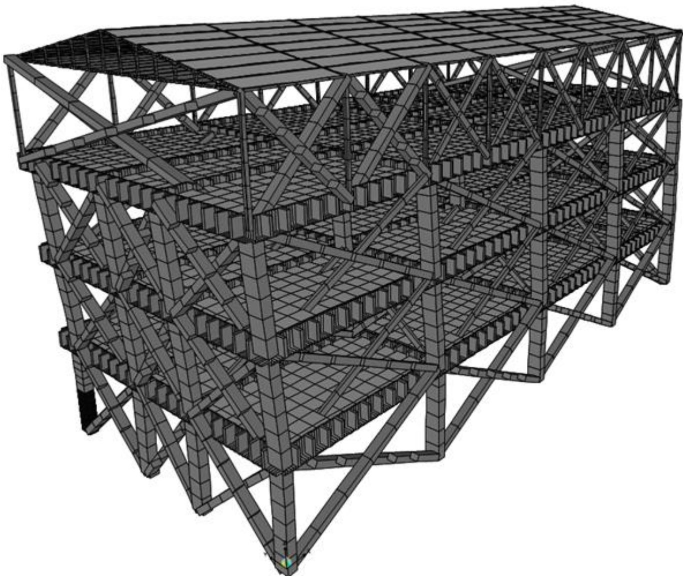

Fig. 13. Revised finite element model of the building

Several sources of uncertainty may influence the reliability of the results presented in this study. First, the mechanical properties of materials—particularly the concrete compressive strength—were assumed based on visual assessments and typical values, rather than core tests or on-site verification, which may affect the accuracy of the finite element model. Second, the number and placement of accelerometers were limited due to practical constraints, potentially leading to incomplete representation of the global dynamic behavior. Third, the selected MAC threshold (0.90) affects mode matching sensitivity; a lower or higher threshold could yield different pairing results. While these factors do not invalidate the conclusions, they introduce a degree of uncertainty that should be considered in the interpretation of the findings. Future studies incorporating more detailed material characterization, denser sensor layouts, and sensitivity analyses of MAC thresholds are encouraged to further reduce these uncertainties.

4. Conclusions

Data collection and finite element model creation phases of seismic performance assessment of a four-storey educational building located in the Yakutiye district of Erzurum, in eastern Türkiye, were assessed in this study. Data was collected in accordance with RYTEIE-2019, a finite element model was created, and theoretical modal analysis was carried out. As a result of this analysis, the calculated natural vibration period to be used in the earthquake load calculation was found to be 1.220 seconds, which was considered to be relatively high for a low-rise reinforced concrete building, and the result was further examined through the results of OMA. The in-situ modal behaviour was experimentally determined through OMA application. Based on the work presented in this research, the following conclusions have been reached:

- It was concluded that the structural contributions of infill walls to the system's rigidity need to be incorporated into the finite element model of low-rise reinforced concrete buildings to accurately assess seismic risks in accordance with the RYTEIE-2019 rules. Considering the consensus in the relevant literature regarding the effects of infill walls, it is believed that the finite element model created by incorporating these effects will better represent the existing structure and allow for a technically more sound evaluation.

- It was demonstrated that the modal behavior parameters of a low-rise reinforced concrete building can be experimentally determined using OMA applications. The relatively small volume of the building, coupled with environmental vibrations (e.g., traffic vibrations, human movement within the structure, etc.), allowed the building to be adequately excited, enabling the automatic extraction of mode shapes through response vibration measurements.
- In OMA applications on the low-rise reinforced concrete building, it was observed that modal behavior parameters could be easily obtained through the analysis of response vibration measurements of 100 Hz sampling frequency. Besides total measurement duration being equal to 500 times the theoretical natural vibration period was found to be adequate.
- It was concluded that an OMA application that involves response vibration measurements at all points determined from theoretical modal analysis would not only provide modal behavior characteristics of the structure but also may supply valuable data regarding the structure's health. This type of OMA application also allowed for the detection and examination of interventions made to the structure, beyond its original state. However, this application was deemed to be time-consuming and required the use of a large number of sensors.
- It is recommended to incorporate OMA applications into the seismic risk assessment of existing reinforced concrete buildings. By reflecting the dynamic behavior characteristics and structural health data obtained through OMA into the finite element model, and conducting structural analyses on the updated model, a much more realistic approach to performance evaluation can be achieved.
- One of the important limitations of this study is the exclusion of potential cracking in infill walls, which could significantly alter the stiffness distribution and, consequently, the fundamental period of the structure. Cracking may reduce the lateral stiffness contribution of infill walls, leading to longer vibration periods and different seismic demand estimations. Additionally, since the analysis was conducted on a low-rise, four-story building, the direct applicability of the results to mid- and high-rise structures is limited. Structural behavior, especially in terms of modal characteristics and infill wall interaction, may differ considerably in taller buildings. These aspects highlight the need for further research to validate and extend the findings to a broader range of structural typologies.
- Certain sources of uncertainty, such as assumptions about material properties, sensor limitations, and the MAC threshold selection, may have influenced the results. These factors have been qualitatively considered to support the reliability of the conclusions.

Declaration of conflicting interests

The author(s) declared no potential conflicts of interest with respect to the research, authorship, and/or publication of this article.

Funding

No funding was received for this study.

Data availability statement

The datasets generated and/or analyzed during the current study are available from the corresponding author on reasonable request.

References

[1] Statista. Development of the Number of Earthquakes Worldwide Since 2000. https://www.statista.com/statistics/263105/development-of-the-number-of-earthquakes-worldwide-since-2000/. Accessed 16 Feb 2025.

[2] AFAD. Event Catalog. https://deprem.afad.gov.tr/event-catalog. Accessed 17 Feb 2025.

[3] Directorate of Communications (2025) Construction and Revival. Presidency of the Republic of Turkey. https://www.iletisim.gov.tr/images/uploads/dosyalar/Ihya_ve_Insa.pdf. Accessed 20 Feb 2025.

[4] Akıncı AC, Ünlügenç UC (2023) The February 6, 2023 Kahramanmaraş earthquakes: Field geological data, evaluation, and impacts on Adana. J Fac Eng Çukurova Univ 38(2):553–569.

[5] Sabırsız E, Şöhret M (2024) Macroeconomic, social, and environmental effects of the February 6 earthquakes on the Turkish economy. J Acad Approaches 15(1):571–597. https://doi.org/10.54688/ayd.1390984.

[6] Tozlu S (2000) Earthquakes in the history of Erzurum. In: Natural Disasters and Earthquakes in Anatolia Throughout History Seminar. Istanbul University Faculty of Literature, History Research Center, Istanbul, Turkey, 22–23 May 2000, pp 93–117.

[7] Aslan Ö (2015) The Effect of Local Soil Conditions on Structural Damage of the March 13, 1992 Erzincan Earthquake. MSc Thesis, Istanbul Technical University, Institute of Science. (In Turkish)

[8] AFAD Erzurum IRAP (2025) Erzurum Provincial Risk Reduction Plan (IRAP). https://erzurum.afad.gov.tr/kurumlar/erzurum.afad/IRAP/Erzurum_IRAP.pdf. Accessed 20 Feb 2025.

[9] Gültekin H, Soyoz S (2023) Experimental and analytical modal analysis of a low-rise RC school building. Bull Earthq Eng 21(2):785–805. https://doi.org/10.1007/s10518-023-01567-9.

[10] Rahmani I, Khajehdehi R (2022) Model updating of existing RC frames using ambient vibration data. Eng Struct 266:114454. https://doi.org/10.1016/j.engstruct.2022.114454.

[11] Demir A, Dönmez C (2024) Evaluation of seismic response of low-rise RC buildings through OMA-based finite element calibration. Soil Dyn Earthq Eng 172:107209. https://doi.org/10.1016/j.soildyn.2024.107209.

[12] Regulation on the Implementation of Law No. 6306 (2019) Regulation on the Identification, Transformation, and Other Relevant Aspects of Risky Buildings (RYTEIE). https://www.mevzuat.gov.tr/mevzuat?MevzuatNo=16849&MevzuatTur=7&MevzuatTertip=5. Accessed 20 Feb 2025.

[13] Law No. 6306 Law on the Transformation of Areas Under Disaster Risk. https://www.mevzuat.gov.tr/mevzuat?MevzuatNo=6306&MevzuatTur=1&MevzuatTertip=5. Accessed 20 Feb 2025.

[14] TBEC (2018) Turkish Building Earthquake Code – Principles for the Design of Buildings Under Earthquake Effects. http://www.resmigazete.gov.tr/eskiler/2018/03/20180318M1-2-1.pdf. Accessed 10 Sep 2018.

[15] SAP2000-V21 (2021) SAP2000 Version 21. Computers and Structures, Inc., Erzurum Technical University.

[16] TS498 (2021) Turkish Standard for the Design and Construction of Reinforced Concrete Structures. Turkish Standards Institution.

[17] Au S-K (2017) Operational Modal Analysis: Modeling, Bayesian Inference, Uncertainty Laws. Springer, Cham.

[18] Rainieri C, Fabbrocino G (2014) Operational Modal Analysis of Civil Engineering Structures: An Introduction and Guide for Applications. Springer, Berlin.

[19] Qin Q, Li HB, Qian LZ, Lau C-K (2001) Modal identification of Tsing Ma Bridge by using improved eigensystem realization algorithm. J Sound Vib 247:325–341. https://doi.org/10.1006/jsvi.2001.3751.

[20] Faecke A, Parolai S, Kling SM, Stempniewski L (2006) Assessing the vibrational frequencies of the Cathedral of Cologne (Germany) by means of ambient seismic noise analysis. Nat Hazards 38:229–236. https://doi.org/10.1007/s11069-005-8616-2.

[21] Romero M, Pachón P, Compán V, Cámara M, Pinto F (2018) Operational modal analysis: A tool for assessing changes on structural health state of historical constructions after consolidation and reinforcement works—Jura Chapel (Jerez de la Frontera, Spain). Shock Vib 2018:3710419. https://doi.org/10.1155/2018/3710419.

[22] Jacobsen NJ, Andersen P (2008) Operational modal analysis on structures with rotating parts. In: Proceedings of the ISMA Conference: International Conference on Noise & Vibration Engineering, Leuven, Belgium.

[23] Okuyucu D (2020) Tek katlı betonarme bir yapı üzerinde operasyonel modal analiz uygulaması. Dicle Üniversitesi Mühendislik Fakültesi Dergisi 11(3):1407–1419. https://doi.org/10.24012/dumf.731668. (In Turkish)

[24] Artemis Modal Pro (2024) Version 2024. Artemis International, Erzurum Technical University.
[25] Ramos LF, Aguilar R, Lourenco PB (2010) Operational modal analysis of historical constructions Using commercial wireless platforms. Struct Health Monit 10:511–521. https://doi.org/10.1177/1475921710388973.
[26] Maia NMM, Silva JMM, He J, Lieven NAJ, Lin RM, Skingle GW (1997) Theoretical and Experimental Modal Analysis. Research Studies Press Ltd.
[27] Allemang RJ (2003) The modal assurance criterion – twenty years of use and abuse. Sound Vib 37(8):14–23.
[28] Guler K, Yuksel E, Kocak A (2008) Estimation of the fundamental vibration period of existing RC buildings in Turkey utilizing ambient vibration records. J Earthq Eng 12:140–150.
[29] Hatzigeorgiou GD, Kanapitsas G (2013) Evaluation of fundamental period of low-rise and mid-rise reinforced concrete buildings. Earthq Eng Struct Dyn 42:1599–1616.
[30] Asteris PG, Repapis CC, Repapi EV, Cavaleri L (2017) Fundamental period of infilled reinforced concrete frame structures. Struct Infrastruct Eng 7:929–941.
[31] Yiğit A, Erdil B, Akkaya İ (2021) A simplified fundamental period equation for RC buildings. Građevinar 73(5):483–497. https://doi.org/10.14256/JCE.3080.2020.
[32] Kose MM (2009) Parameters affecting the fundamental period of rc frame with infill walls. Eng Struct 39:93–102.
[33] Koçak A, Yıldırım MK (2011) Effects of infill wall ratio on the period of reinforced concrete framed buildings. Adv Struct Eng 14(5):731–743. https://doi.org/10.1260/1369-4332.14.5.731.
[34] Earthquake Hazard Map of Turkey. https://tdth.afad.gov.tr/. Accessed 3 Feb 2025.
[35] Federal Emergency Management Agency (FEMA) (2000) Prestandard and Commentary for the Seismic Rehabilitation of Buildings (FEMA 356). FEMA, Washington, DC.